16th World Conference on Earthquake, 16WCEE 2017

Santiago Chile, January 9th to 13th 2017

Paper N° 431

Registration Code: S-C1462401885

Damage balance of asymmetric structures with nonlinear behavior by means of a tuned mass damper

Gilda Espinoza[1], José Luis Almazán[2], Diego Neira[1], José Norambuena-Contreras[1]

[1] *Department of Civil and Enviromental Engineering, University of Bio-Bio, Concepción, Chile.*

[2] *Department of Structural and Geotechnical Engineering, Pontificia Universidad Católica de Chile, Santiago, Chile.*

Abstract

This research studies the effectiveness of a tuned mass damper (TMD) to balance the structural damage on asymmetric nonlinear structures subjected to a unidirectional seismic movement. Using the statistical and equivalent linearization technique, a model with three resistant planes with nonlinear behavior (oriented in the direction of the seismic movement) has been analyzed with a linear TMD. The nonlinear constitutive law of each resistant plane is represented by a Bouc-Wen element. The hysteretic energy of each plane normalized with respect to a symmetric structure without TMD is used as damage index, and it is equaled on the three planes to balance the damage over the asymmetric system. The design parameters of the TMD are obtained by equaling the hysteretic energy on the three planes. The results show that optimum response of the structure with TMD is very sensitive both to the frequency and the device position, and not to the damping of the TMD. In the case of structures subjected to an input of broad-bandwidth, the TMD tends to synchronize with the equivalent uncontrolled linear frequency, where dominates the deformation at the edge of maximum response. In contrast, for an excitation of narrow-bandwidth the optimum frequency of the TMD synchronizes with the dominant frequency of the excitation. Moreover, in broad-bandwidth processes, the TMD optimal location is over the edge with larger deformations under the uncontrolled condition, while for long period structures subjected to narrow-bandwidth excitations, the TMD locates on the rigid edge. These positions are coincident with the edge where the most damaged plane is located, without TMD. In the case of broad-bandwidth processes balance of damage can only be achieved with low values of eccentricity (on average $e_s/r < 0{,}1$), which is coincident with the position threshold condition of TMD within the floor section. Besides, in broad-bandwidth processes, as the inelastic incursion increases, the optimum frequency of the TMD decreases, while for narrow-bandwidth processes the TMD tunes the predominant frequency of the input, independently of the level of nonlinearity of the structure. Also, results suggest that increasing the nonlinearity level of the structure, the damage is simultaneously reached for a wide range of eccentricities. In general, the condition of uniform distribution of the damage normalized with respect to the symmetric system does not lead to a uniform reduction regarding the asymmetric system without TMD, being both the damage and the inelastic deformations lower over the plane closest to the location of the damper, thus producing an amplification in the rest of planes. Finally, the results show that for structures with decoupled torsional frequency ratio equal to 1, a natural balance of the reduction of hysteretic energy and the deformations with respect to the asymmetric system without TMD take place.

Keywords: Structural damage; Hysteretic energy; Tuned Mass Damper; Nonlinear structures; Bouc-Wen hysteretic model; Statistical and equivalent linearization.

1. Introduction

Tuned Mass Dampers (TMDs) are devices used to control vibrations in structures. A TMD consists on a secondary mass connected with the main system using a spring and a damper, which dissipate the vibratory energy through relative displacement between the main system and the device. Their effectiveness in vibrations control caused by wind and low-intensity seismic movements is widely accepted [1-3]. However, their performance under high seismic loads heavily depends on the seismic movement characteristics [4].

Previous researches considered the main system as an elastic system, although advances in structural design techniques have established the need to extend research about structures with non-linear behavior. This is because structures are designed to be damaged by high-intensity seismic events. In this context, several researchers [5-8] have studied the behavior of symmetric and inelastic structures with a linear TMD. The purpose of these researches was to improve the response of the main structure subjected to a seismic event, although different parameters can be used to measure the effectiveness of a TMD. The most commonly used criteria are based on theoretical damage indexes, which establish the damage of a structure using a balance between maximum deformation of structural element and dissipated hysteretic energy. In general, these results show that TMD can slightly reduce the structure displacement peak after creep, but it can also significantly reduce damage of the structure through dissipated hysteretic energy. Moreover, above mentioned structures considered a symmetric main structure, that is, the center of mass of the structure coincides with the center of stiffness of the structure. However, this criterion does not match with structural design practices where usually asymmetric structures are built as result of architectural or economic considerations.

In this context, first study carried out concerning this issue [9] concluded that effectiveness of Multiple Tuned Mass Dampers (MTMDs) to control lateral response of torsionally coupled systems decreases with the degree of asymmetry. Based on this study, several researches have been carried out with the objective of measuring effectiveness of TMDs on multi-storey [9-12] or one-floor [8, 11, 12, 14] buildings. In short, design parameters of TMDs for asymmetric structures considered in these studies were the following: optimal location, optimal frequency and optimal damping. These parameters arise as a result of minimizing different objective functions, such as: ratio between displacement root mean square and rotation of the system with TMD compared with the system without TMD [9], ratio between square mean of the displacement response in controlled mode of buildings with and without TMD [10] or a particular response of the structure like floor accelerations, inter-story drifts and base shear, amongst others [11, 12, 14].

Additionally, another criteria to torsional control of structures is torsional balance [13, 15-17]. This concept establishes that reducing lateral and torsional displacements together with the correlation degree between them is necessary. This is achieved by equalizing deformation demand of structure edges. Most of researches about asymmetric structures have been carried out to study main linear systems, meanwhile the study about non-linear structures has been focused on torsional balance concept [13,17]. Thus, the ability of TMD devices to decrease damage of asymmetric structures with non-linear behavior reducing the hysteretic energy dissipated by structural elements has not been studied nowadays.

For all these reasons, the objective of this work is to analyze the ability of a TMD to balance the damage of an asymmetric structure with non-linear behavior against a seismic event, considering this balance of damage as the equality of hysteretic energy dissipated by the structural elements. With this purpose, optimal parameters of TMD have been determined based on the damage balance optimization criterion. To do this, a structural model subjected to a broad-band process (BBP) that corresponds to an accelerogram compatible with the Chilean Standard NCh 2745 for firm soil, and to a narrow-band process (NBP) correspondent with the 1985 Mexico DF earthquake recorded in North-South direction, has been used. Hence, a parametric analysis on three variables has been carried out: (1) eccentricity of the structure, (2) reduction factor and (3) ratio of torsional frequency. Finally, last part of the study analyzes the influence of TMD on the dissipated energy and on the deformation demand of structure edges comparing the asymmetric structure with and without TMD.

2. Structural model and equations of motion

A one-storey mono-symmetric structural model subjected to a one-directional seismic load has been considered in this research. This model has three nonlinear resisting planes located in the seismic input direction (see Fig. 1). Side length ratio is $a/b = 4$, where the Geometric Center (CR) is coincident with the Center of Stiffness (CS), and the Center of Mass (CM) is located at a distance "e_s" from CR.

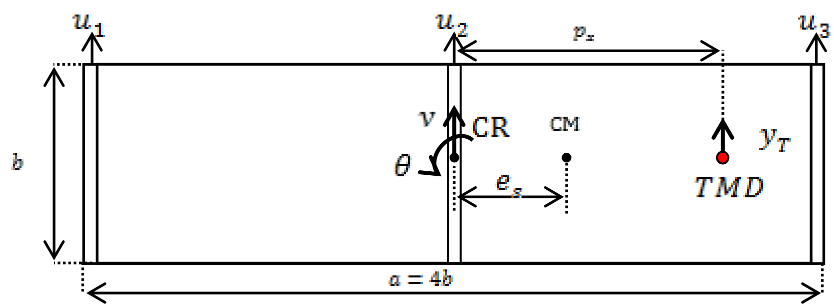

Fig. 1. Mono-symmetric structural model used in the study.

Non-linear behavior of each resisting plane is represented by a Bouc-Wen element. Therefore, the equations of motion of the system can be written as:

$$\mathbf{M}\ddot{\mathbf{q}} + \mathbf{C}\dot{\mathbf{q}} + \mathbf{L}_\mathbf{f}^\mathbf{T}\mathbf{f}_\mathbf{nl} + \mathbf{L}_\mathbf{t}^\mathbf{T} f_t = -\mathbf{M}\mathbf{R}\ddot{u}_g \tag{1}$$

$$\mathbf{M} = \begin{bmatrix} \mathbf{M}_s & \mathbf{0}_{2x1} \\ \mathbf{0}_{1x2} & m_t \end{bmatrix} \mathbf{M}_s = m_s \begin{bmatrix} 1 & e_s \\ e_s & r_s^2 \end{bmatrix} \quad \mathbf{C} = \begin{bmatrix} \mathbf{C}_s & \mathbf{0}_{2x1} \\ \mathbf{0}_{1x2} & 0 \end{bmatrix} + \mathbf{L}_\mathbf{t}^\mathbf{T} c_t \mathbf{L}_\mathbf{t} \tag{2}$$

$$\mathbf{L}_\mathbf{t} = \begin{bmatrix} -1 & -p_x & 1 \end{bmatrix} \quad \mathbf{L}_\mathbf{f} = \begin{bmatrix} 1 & -a/2 & 0 \\ 1 & 0 & 0 \\ 1 & a/2 & 0 \end{bmatrix} \quad f_t = k_t u_t \tag{3}$$

where $\mathbf{q}(\mathbf{t}) = [y(t) \quad \theta(t) \quad y_t(t)]^T$ is the degrees of freedom vector of the system; $y(t)$ is the lateral displacement of CR in the Y direction; $\theta(t)$ is the rotation of the floor; $y_t(t)$ is the TMD displacement with respect to ground; $\mathbf{R} = [1 \quad 0 \quad 1]^T$ is the incidence vector of the seismic input; $\mathbf{M}_s$ is the mass matrix of the main structure; m_s is the translational mass and $r_s = \sqrt{(a^2+b^2)/12}$ is the floor radius of gyration; $\mathbf{C}_s$ is the damping matrix assuming a constant damping ratio of $\xi_s = 0.05$; and finally, e_s is the structural eccentricity defined as the distance between CR and CM.

Regarding to Bouc-Wen model, z corresponds to the hysteretic variable; $\alpha_s, \beta, \lambda, \gamma$ and η are the hysteretic model parameters; and F_y and ΔY are the force and creep displacement of resisting planes, respectively.

$$f_{nl_j} = \alpha_{sj}\frac{F_{yj}}{\Delta Y_j}u_j + \left(1-\alpha_{sj}\right)F_{yj}z_j \qquad j = 1{:}3 \tag{4}$$

$$\dot{z}_j = \frac{1}{\Delta Y_j}\dot{u}_j\left(\lambda - \left|z_j\right|^{\eta}\left(\beta + \gamma \mathrm{sgn}\left(z_j\right)\mathrm{sgn}\left(\dot{u}_j\right)\right)\right) \tag{5}$$

3. Seismic excitation

Ground motion as a limited bandwidth stationary random process has been considered to the development of this study. Fig. 2(a) represents a broad-band random process compatible with the Chilean Standard NCh 2745 for type 2 of firm soil. Moreover, Fig. 2(b) presents a narrow-band process obtained from the 1985 Mexico DF earthquake recorded in the North-South direction. In both cases, the power spectral density (PSD),$S_g(\omega)$, adjusted to the modified Kanai-Tajimi filter is defined according to Eq. (6):

$$S_g(\omega) = S_0\frac{\omega_g^4 + 4\xi_g^2\omega_g^2\omega^2}{\left(\omega_g^2-\omega^2\right)+4\xi_g^2\omega_g^2\omega^2}\frac{\omega^4}{\left(\omega_f^2-\omega^2\right)^2+4\xi_f^2\omega_f^2\omega^2} \tag{6}$$

whereS_0, ω_g, ξ_g, ω_f and ξ_f are the parameters adjusted by the least-squares method.

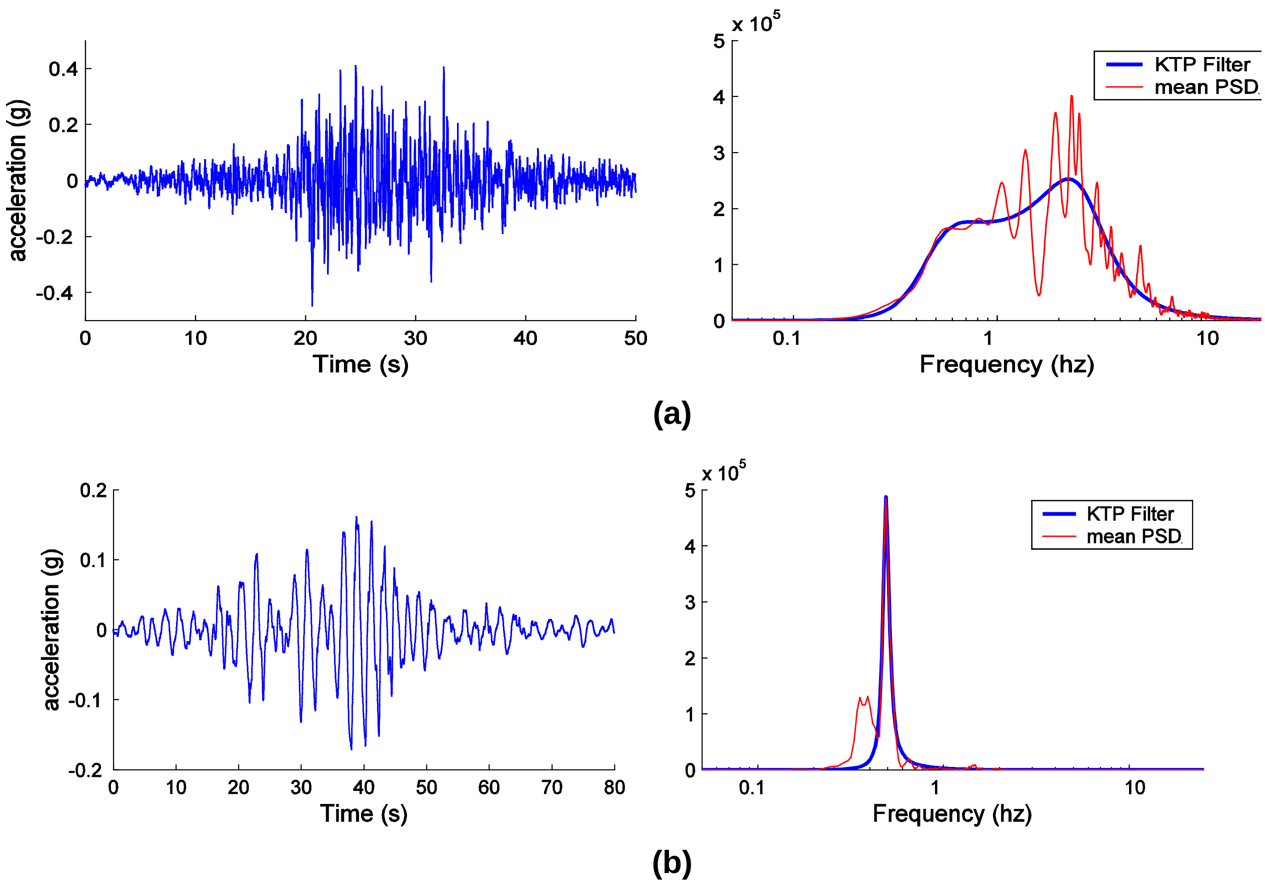

Fig. 2. Seismic excitations considered: (a) broad-band process compatible with Chilean Standard NCh 2745 for type 2 soil, and (b) narrow-band process registered from 1985 Mexico DF earthquake (SCT).

4. Equivalent statistical linearization

Equivalent statistical linearization method has bee n used to solve the non-linear differential equations of motion. This method transforms the system with non-linear hysteretic behavior in a linear system replacing Eq. (5) by a linear equation:

$$\dot{z} = -K_{eq}\left(\mathbf{V_q}, t\right)z - C_{eq}\left(\mathbf{V_q}, t\right)\dot{u} \tag{7}$$

where K_{eq} and C_{eq} are coefficients dependent on the covariance matrix $\boldsymbol{V}_q$:

$$K_{eq} = \sqrt{\frac{2}{\pi}}\beta\left[\sigma_{\dot{u}} + \frac{\gamma_{\dot{u}z}}{\sigma_z}\right] \quad C_{eq} = \sqrt{\frac{2}{\pi}}\beta\left[\sigma_z + \frac{\gamma_{\dot{u}z}}{\sigma_{\dot{u}}}\right] - 1 \tag{8}$$

where σ_z and $\sigma_{\dot{x}}$ are z and $\dot{x}$ standard deviations, respectively; and $\gamma_{\dot{x}z}$ is cross-covariance between $\dot{x}$ and z. Besides, covariance matrix $\boldsymbol{V}_q$ associated to vector $\mathbf{q(t)}$ can be calculated as:

$$\mathbf{V_q} = E\{\mathbf{q(t)q(t)^T}\} = \frac{1}{2\pi}\int_{-\infty}^{\infty}\mathbf{H_q}(j\omega)S_g(\omega)\mathbf{H_q^*}(j\omega)d\omega \tag{9}$$

where $E\{\cdot\}$ represents the expected value of the process considering that $\mathbf{H}_q(j\omega)$ is the frequency response matrix and $\mathbf{H}_q^*(j\omega)$ its conjugated-transpose matrix.

As it can be concluded, equivalent linearization is an iterative process, because it is necessary to know K_{eq} and C_{eq} to calculate the covariance matrix, and these coefficients also depend on the standard deviations σ_z and $\sigma_{\dot{x}}$.

5. Balance of damage

As was mentioned in the introduction section, main objective of this work is to balance the damage of a non-linear asymmetric structure by means of a TMD, evaluating damage trough the hysteretic energy dissipated by the resisting planes. Therefore, once the covariance matrix is calculated, damage of the resisting planes can be determined using Eq. (10), which calculates average value of the dissipated energy by each plane,

$$\langle e_h\rangle = (1-\alpha_s)\omega_s^2\int_0^T \gamma_{\dot{u}z}(\tau)d\tau = (1-\alpha_s)\omega_s^2\gamma_{\dot{u}z}T \tag{10}$$

where T is the duration of the excitation process considered. This is calculated for the three resisting planes of the structure, obtaining the vector that represents the energy dissipated by the structure $\mathbf{F}$.

$$\mathbf{F} = \begin{Bmatrix}(1-\alpha_{s1})\omega_s^2\gamma_{\dot{u}z1}T\\(1-\alpha_{s2})\omega_s^2\gamma_{\dot{u}z2}T\\(1-\alpha_{s3})\omega_s^2\gamma_{\dot{u}z3}T\end{Bmatrix} \tag{11}$$

Finally, the optimization problem consists on equaling the energy dissipated by the planes, which can be achieved maximizing the dissipated energy vector of the structure, by minimizing the damage functional (J) through TMD parameters.

$$\text{Minimize: } J(\omega_d, p_x, \xi_d) = \text{Max}\,(\mathbf{F}) \quad \text{s/a} \quad -a/2 < p_x < a/2 \qquad \omega_t > 0 \tag{12}$$

6. Results and discussion

A sensitivity analysis of TMD parameters at the structure response was carried out. To do this, Fig. 3 shows contour lines of the damage functional for model structure with parameters $T_s = 2.5\ s$, $e_s/r_s = 0.3$, $\xi_s = 0.05$, $\Omega_s = [0.7, 1.0, 1.3]$, $\mu = 0.02$, $R = 5$, $n = 1$ and $\alpha_1 = \alpha_2 = \alpha_3 = 0.5$ subjected to a broad-band process. The upper row shows contour lines for $\xi_d = \xi_d^{(op)}$, middle row for $p_x = p_x^{(op)}$ and the lower row for $\omega_d = \omega_d^{(op)}$. In this Figure, it can be observed that optimal solution is very sensitive both to the frequency and the device position, but not to the damping factor. Due to that, a constant value of damping was assumed, $\xi_d = 0.12$.

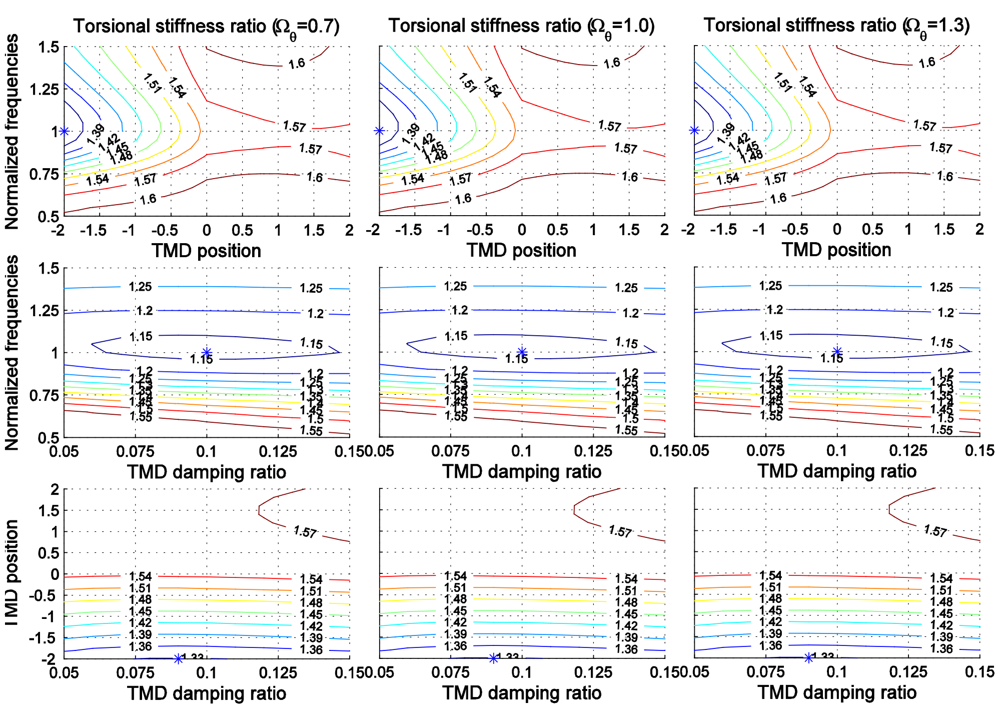

Fig. 3. Contour lines of the functional J for the structure subjected to a BBP ($\boldsymbol{T_s = 2.5\ s}$, $\boldsymbol{e_s/r_s = 0.3}$, $\boldsymbol{\xi_s = 0.05}$, $\boldsymbol{\Omega_s = [0.7, 1.0, 1.3]}$, $\boldsymbol{\mu = 0.02}$, $\boldsymbol{R = 5}$, $\boldsymbol{n = 1}$ and $\boldsymbol{\alpha_1 = \alpha_2 = \alpha_3 = 0.5}$)

Additionally, Fig. 4 and Fig. 5 present optimum position of TMD. Fig. 4 shows the results of the model with parameters $T_s = 2$, $\xi_s = 0.05$, $\Omega_s = [0.7, 1.0, 1.3]$, $\mu = 0.02$, $R = 5$, $n = 1$ and $\alpha_1 = \alpha_2 = \alpha_3 = 0.5$, subjected to broad-band and narrow-band processes. The upper row shows the results obtained for the optimum frequency of TMD normalized with respect to ω_s and the equivalent linear natural frequencies of the structure without TMD. The lower row presents the optimum position of TMD normalized with respect to width, $p_x^{(op)}/a$. It can be appreciated that in the case of BBPs the optimum frequency tends to tune with linear equivalent frequencies associated to the predominant mode. In contrast, in the case of NBPs the optimum frequency of TMD tends to tune with the dominant frequency of the seismic input, that is $\omega_i = \pi\ (T_i = 2\ s)$, where the excitation energy concentrates. Regarding the optimum position, it can be observed that in the case of torsionally flexible structures TMD tends to locate at the rigid edge, while in the case of torsionally rigid structures optimum position locates at the flexible edge.

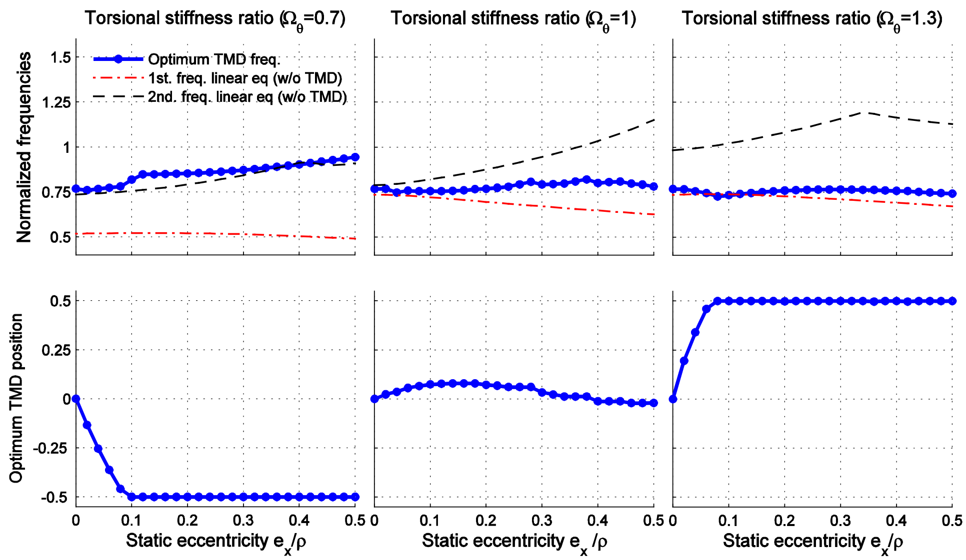

(a)

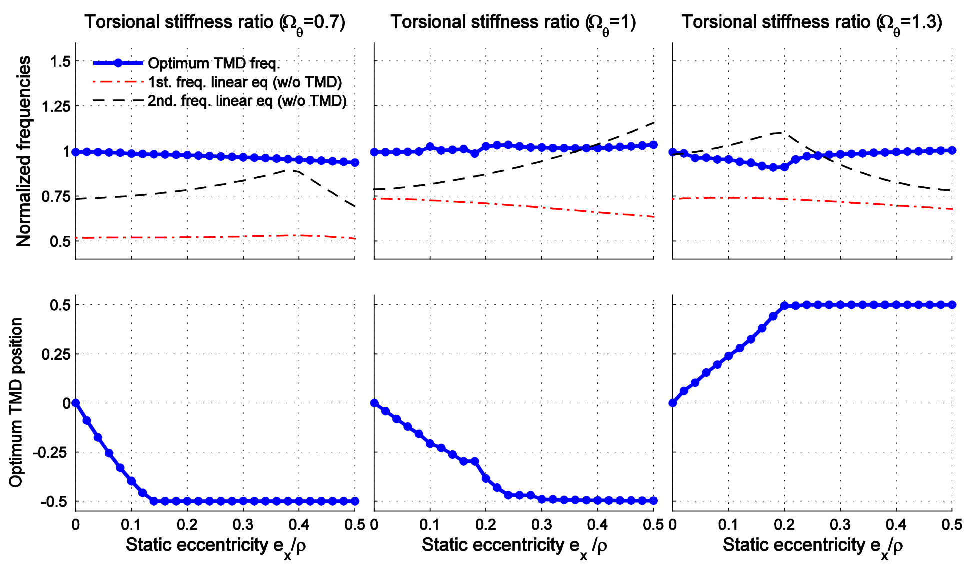

(b)

Fig. 4. Frequency and optimum position of TMD: (a) BBP and (b) NBP. Structure model ($\boldsymbol{T_s = 2, \xi_s = 0.05}$, $\boldsymbol{\Omega_s = [0.7, 1.0, 1.3]}$, $\boldsymbol{\mu = 0.02}$, $\boldsymbol{R = 5}$, $\boldsymbol{n = 1}$ and $\boldsymbol{\alpha_1 = \alpha_2 = \alpha_3 = 0.5}$).

Additionally, Fig. 5 shows the results of the model with parameters $T_s = 1.5, \xi_s = 0.05$, $\Omega_s = [0.7, 1.0, 1.3]$, $\mu = 0.02$, $e_s/r_s = 0.3$, $n = 1$ and $\alpha_1 = \alpha_2 = \alpha_3 = 0.5$, subjected to broad-band and narrow-band processes. In this Figure, results are presented as a function of the reduction factor. As it happened before, in the case of BBP optimum frequency tends to tune with the uncontrolled linear equivalent frequency. However, with a higher reduction factor, minimum decrease of the TMD optimum frequency can be observed.

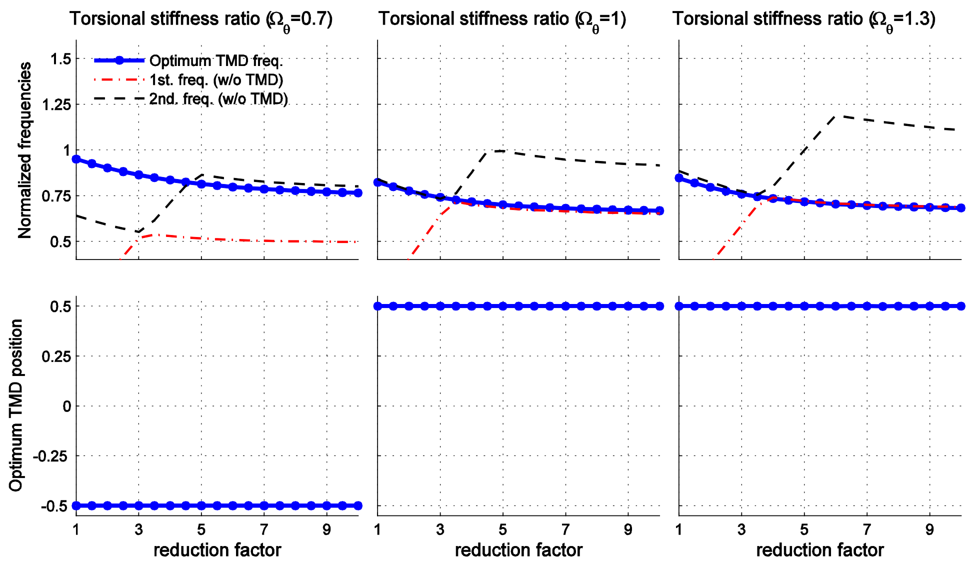

(a)

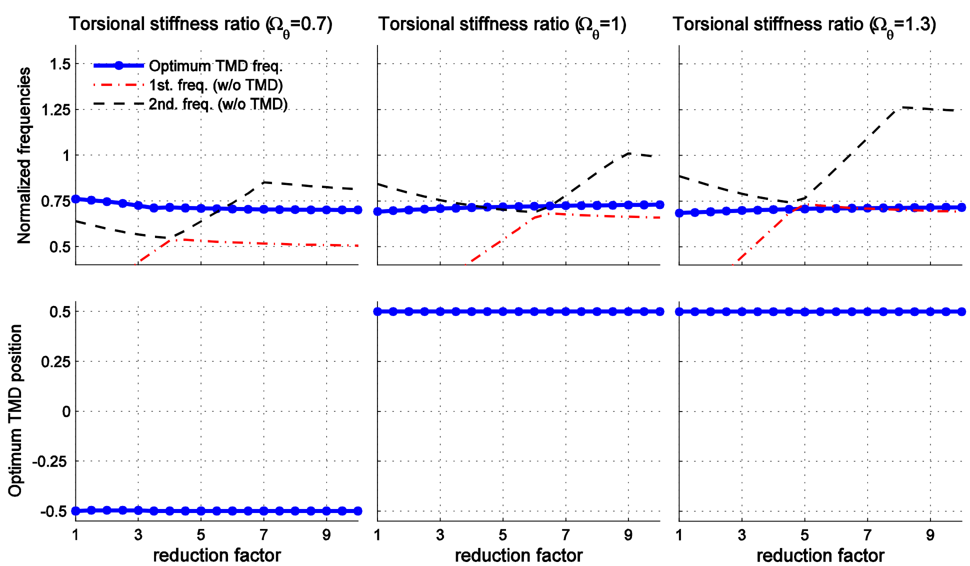

(b)

Fig. 5. Frequency and optimum position of TMD (a) BBP and (b) NBP. Structure model ($\boldsymbol{T_s = 1.5}$, $\boldsymbol{\xi_s = 0.05}$, $\boldsymbol{\Omega_s = [0.7, 1.0, 1.3]}$, $\boldsymbol{\mu = 0.02}$, $\boldsymbol{e_s/r_s = 0.3}$, $\boldsymbol{n = 1}$ and $\boldsymbol{\alpha_1 = \alpha_2 = \alpha_3 = 0.5}$).

Moreover, Fig. 6 presents hysteretic energy dissipated by the structure and the variance of the edge deformation of the structure with and without TMD normalized with respect to the symmetric structure, in the case of the model structure with parameters $T_s = 2, \xi_s = 0.05$, $\Omega_s = [0.7,1.0,1.3]$, $\mu = 0.02$, $R = 5$, $n = 1$ and $\alpha_1 = \alpha_2 = \alpha_3 = 0.5$, and subjected to BBP and NBP. The upper row shows the results of the dissipated symmetric hysteretic energy and the lower row shows the variance of the edge deformation. It can be appreciated in these Figures that in the case of torsionally stiff and flexible structures TMD achieves to balance damage of the structure for small eccentricity values both in BBP and NBP. It also achieves to equate the variance of the edge deformation. In contrast, in torsionally hybrid structures the damage balance can be achieved with wider ranges of eccentricity specially when subjected to NBP.

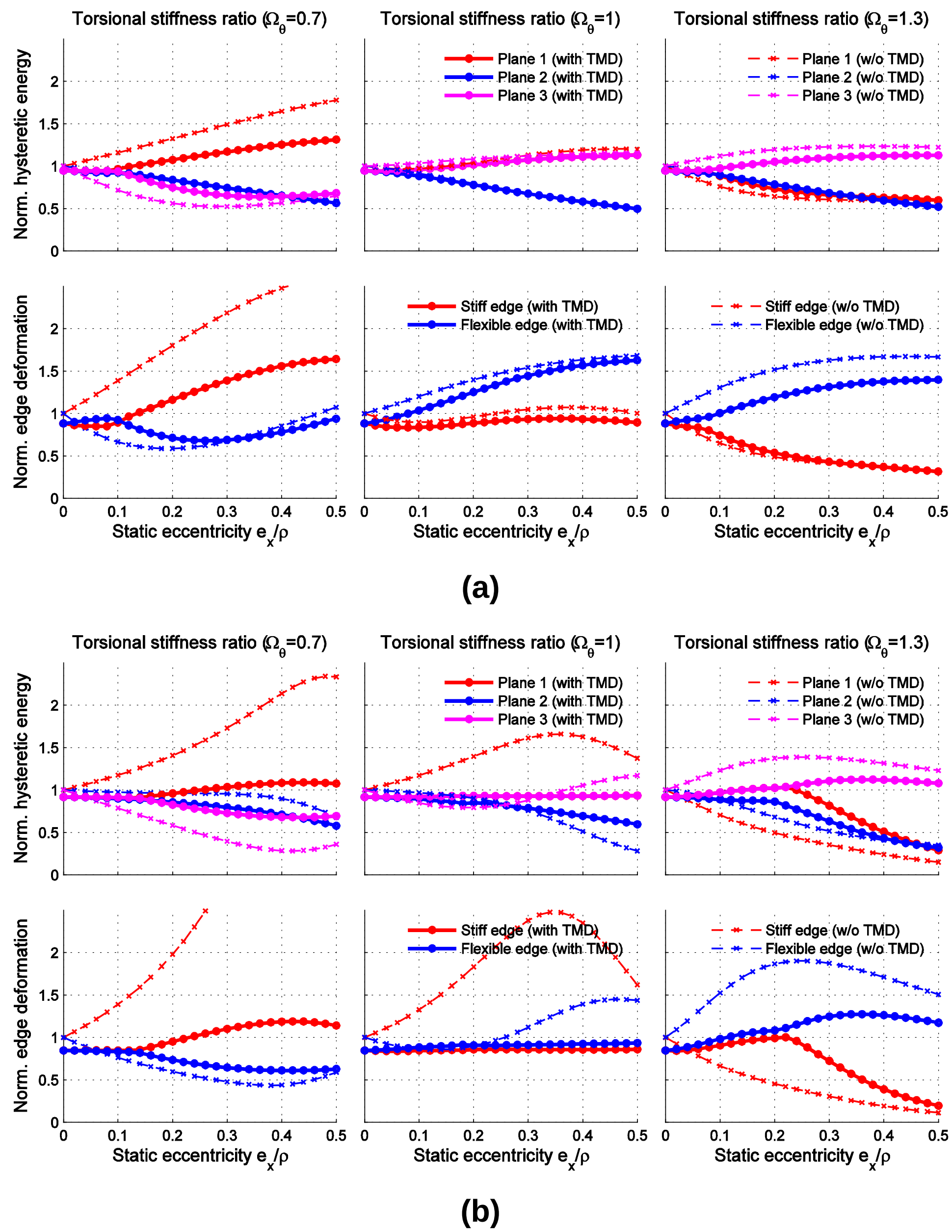

Fig. 6. Energy and variance of normalized edge deformations: (a) BBP and (b) NBP. Structure model ($\boldsymbol{T_s = 2, \xi_s = 0.05, \Omega_s = [0.7, 1.0, 1.3], \mu = 0.02, R = 5, n = 1}$ and $\boldsymbol{\alpha_1 = \alpha_2 = \alpha_3 = 0.5}$).

Finally, Fig. 7 presents ratios of energy and variance of the edge deformation of the structure with TMD vs the structure without TMD, for the model structure with parameters $T_s = 2, \xi_s = 0.05$, $\Omega_s = [0.7, 1.0, 1.3]$, $\mu = 0.02$, $R = 5$, $n = 1$ and $\alpha_1 = \alpha_2 = \alpha_3 = 0.5$, subjected to BBP and NBP. The upper row shows energy ratio and lower row shows variance of edge deformation ratio. It can be seen that TMD achieves to reduce both the dissipated energy and the variance of deformation of its nearest plane. In contrast, the opposite plane undergoes an increase of these values.

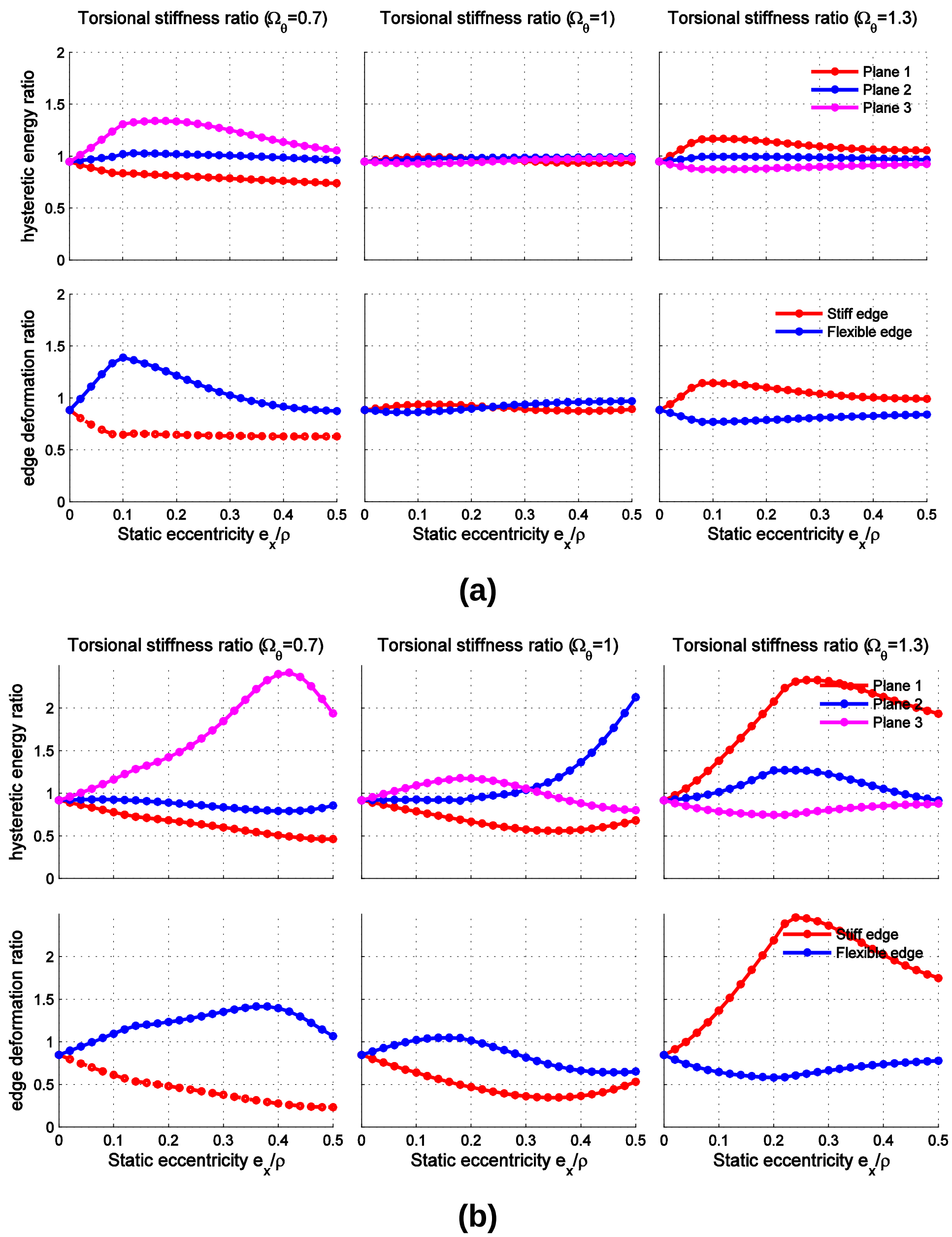

Fig. 7. Ratios of energy and variance of edge deformations ($^{w}TMD/^{w/o}TMD$) (a) BBP and (b) NBP. Structure model ($T_s = 2, \xi_s = 0.05, \Omega_s = [0.7, 1.0, 1.3]$, $\mu = 0.02$, $R = 5$, $n = 1$ and $\alpha_1 = \alpha_2 = \alpha_3 = 0.5$).

7. Conclusions

Based on the main results obtained from this research, the following conclusions have been extracted:

1. In the case of BBP, TMD tends to tune with the uncontrolled equivalent linear frequency associated to the predominant mode, while in the case of NBP, optimum frequency of TMD tends to tune with the dominant frequency of the seismic excitation.
2. The optimum position of TMD tends to locate at the edge with the highest damage in the case of the structure without TMD.
3. The optimum response of the structure without TMD is very sensitive both to the frequency and the device position, but not to the damping factor of the TMD.

4. Damage can be balanced in resisting planes of the structure only in the case of low eccentricity values (on average $e_s/r < 0{,}1$) , until the TMD position reaches the edge of the floor.
5. In the case of BBPs, the higher the non-linearity degree (higher reduction factor), the lower the optimum frequency of the TMD. In contrast, in the case of NBP the optimum frequency is independent of the non-linearity degree.
6. The implementation of an optimum TMD in a structure reduces the dissipated energy in the plane where the TMD is located, reaching a reduction of up to 20% in the case of BBP processes ($\Omega_s = 0.7$, $e_s/r = 0.5$) and 40% for NBP processes ($\Omega_s = 0.7$, $e_s/r = 0.5$).
7. An optimal TMD in a structure produces an amplification of the energy ratio on the plane located farthest from the TMD of up to 30% for BBP processes ($\Omega_s = 0.7$, $e_s/r = 0.15$) and of up to 250% for NBP processes ($\Omega_s = 0.7$, $e_s/r = 0.4$).
8. The optimum TMD also produces a reduction of the edge deformation in the plane where the TMD is located of up to 40% for BBP processes ($\Omega_s = 0.7$, $e_s/r = 0.1$) and of up to 75% for NBP processes ($\Omega_s = 0.7$, $e_s/r = 0.5$).
9. In structures with an optimum TMD, an amplification of the edge deformation in the plane located farthest from the TMD can be produced, reaching values of up to 40% for BBP processes ($\Omega_s = 0.7$, $e_s/r = 0.1$) and of up to 250% for NBP processes ($\Omega_s = 1.3$, $e_s/r = 0.23$).

8. Acknowledgements

This research has been funded by the National Commission for Scientific and Technical Research (CONICYT) through the Project FONDECYT Nº1120937, and by the University of Bio-Bio trough the Research Project DIUBB 132714 3/R. The authors thank for the economic support.

9. References

[1] Kwok, K., 1995. Performance of tuned mass dampers under wind loads. Engineering Structural, Volume 9, pp. 665-667.

[2] Kaynia, A., Veneziano, D., Biggs, J., 1891. Seismic effectiveness of tuned mass dampers. Journal of Structural Engineering, 107(8), pp. 1465-1484.

[3] Warburton, G., 1982. Optimal absorver parameters for various combinations of response and exciation parameters. Earthquake Engineering & Structural dynamics, Volumen 10, pp. 381-301.

[4] Villaverde, R., 1994. Seismic control of structures with damped resonant appendages. Los Angeles, California, USA, s.n., p. 11.

[5] Soto-Brito, R. & Ruiz & S., 1999. Influence of ground motion intensity on the effectiveness of tuned mass dampers. Earthquake Engineering and Structural Dynamics, Volume 28, pp. 1255-1271.

[6] Pinkaew, T., Lukkunaprasit, P., Chatupote P., 2003. Seismic effectiveness of tuned mass dampers for damage reduction of structures. Engineering Structures, Volume 25, pp. 39-46.

[7] Sgobba, S. & Marano, G., 2010. Optimus design of linear tuned mass damper for structures with nonlinear behaviour. Mechanical Systems and Signal Processing, 26(6), pp. 1739-1755.

[8] Zhang, Z. & Balendra, T., 2013. Passive control of bilinear hysteretic structures by tuned mass damper for narrow band seismic motion. Engineering Structures, Volume 54, pp. 103-111.

[9] Jangid, R. & Datta, T., 1997. Performance of multiple tuned mass dampers for torsionally couple system. Earthquake Engineering and Structural Dynamics, Volume 26, pp. 307-317.

[10] Lin, C. C., Ueng, J. M. & Huang, T. C., 1999. Seismic response reduction of irregular buildings using passive tuned mass dampers. Engineering Structures, Volume 30, pp. 513-524.

[11] Singh, M., Singh, S. & Moreschi, L., 2002. Tuned mass dampers for response control of torsional buildings. Earthquake Engineering and Structural Dynamics, Volume 31, pp. 749-769.

[12] Ueng, J. M., Lin, C. C. & Wang, J. F., 2008. Practical design issues of tuned mass dampers for torsionally coupled buildings under earthquake loadings. The Structural Design of Tall and Special Buildings, Volume 17, pp. 133-165.

[13] Almazán, J. L., Espinoza, G. & Aguirre, J. J., 2012. Torsional balance of asymmetric structures by means of tuned mass dampers. Engineering Structures, Volume 42, pp. 308-328.
[14] Li, C. & Qu, W., 2012. Optimum properties of multiple tuned mass damper for reduction of translational and torsional response of structures subject to ground acceleration. Engineering Structures, Volume 28, pp. 472-494.
[15] De la Llera, J., Almazán, J. & Vial, I., 2005. Torsional balance of plan-asymmetric structures with frictional dampers: analytical results. Earthquake Engineering and Structural Dynamics, Volume 34, pp. 1089-1108.
[16] García, M., De la Llera, J. & Almazán, J., 2007. Torsional balance of asymmetric structures with viscoelastic dampers. Engineering Structures, Volume 29, pp. 914-932.
[17] Espinoza, G., Almazán, J. & Jara, C., 2015. Balance torsional de estructuras asimétricas no lineales por medio de un amortiguador de masa sintonizado. XI Congreso Chileno de Sismología e Ingeniería Sísmica. Santiago, Chile. s.n.